

Article

Microscopic visualization of a granitic rock subject to dynamic tensile loading by using a micro X-ray CT system

S. H. Cho^{*†}, S. Kubota^{**}, Y. Ogata^{**}, M. Yokota^{*}, and K. Kaneko^{*}

^{*}Division of Field Engineering for Environment, Graduate School of Engineering, Hokkaido University, Kita 13, Nishi 8, Sapporo, 060-8628, JAPAN

[†]Present address: Department of civil engineering, University of Toronto, CANADA

^{*}corresponding author: sh.cho@utoronto.ca

^{**}Application and Environmental Protection Team, Research Center for Explosive Safety, National Institute of Advanced Industrial Science and Technology (AIST), 16-1 Onogawa, Tsukuba, 305-8569, JAPAN

Received: May 27, 2005 Accepted: July 28, 2005

Abstract

The dynamic tension test based on Hopkinson's effect together with the spalling phenomena generates numerous cracks in the test specimens, which are due to the dynamic fracture process and rock inhomogeneity. In the dynamic tensile test, the free surface displacement velocity at the free end is measured with a laser vibration meter and the fractured planes are observed using a high-speed camera. The position where the specimen first fractures is selected as the fracture plane. The position of the fracture plane and measured displacement velocities are then used to determine the dynamic tensile strength. Therefore, it is important to verify the mechanism of the fracture plane formation. In this study, micro X-ray CT system is used to visualize the 3-D microstructure of a rock specimen subject to dynamic tensile loading in a nondestructive manner.

Keywords: Microfocus X-ray CT, Dynamic tensile test, Inada granite, Microscopic visualization, Hopkinson's effect

1. Introduction

A dynamic tensile test based on Hopkinson's effect together with the spalling phenomena was used to estimate the dynamic tensile strength of a rock and its strain rate dependency¹⁾⁻³⁾. In the dynamic tensile test, an incident compressive stress wave in a material is reflected as a tensile wave at the free end and at the same time, the reflected wave and the tail of the incident compressive wave are superposed. The superposed wave develops into a tensile stress wave, which in turn generates fractures near the free end of the material. The place where the specimen first fractures was selected as the fracture plane and the tensile stress at the fracture plane was considered the dynamic tensile strength of the material. The dynamic tensile strength shows the strain rate dependency at high strain rate. From this test, we found that the inhomogeneity of rock has a significant effect on the strain rate dependency of the dynamic tensile strength, and numerous cracks parallel to the free end side were generated in the rock specimen³⁾.

X-ray computed tomography (CT) was first introduced in the medical field and is now applied for industrial applications⁴⁾⁻⁶⁾. Recently, high-resolution X-ray CT has been used to observe microstructure of mineral particles and rock samples⁷⁾⁻⁹⁾. In this study, we studied the micro X-ray CT system which was used to conduct microscopic observation of a granitic rock specimen subject to dynamic tension was studied. Information obtained from these observations is important for verifying the dynamic fracture process of rock in tension and the strain-rate dependency of dynamic tensile strength.

2. Micro X-ray computed tomography (CT) system

The custom designed micro X-ray CT system (TOSCANER 30900 μ hd), as shown in Fig. 1, which is installed at Hokkaido University, uses multi-scan and cone geometry to observe three-dimensional microstructure of an object. Figure 2 shows a schematic diagram of the micro CT sys-



Fig. 1 High resolution micro X-ray computed tomography (CT) system (TOSCNAR 30900 μ hd, Toshiba co.).

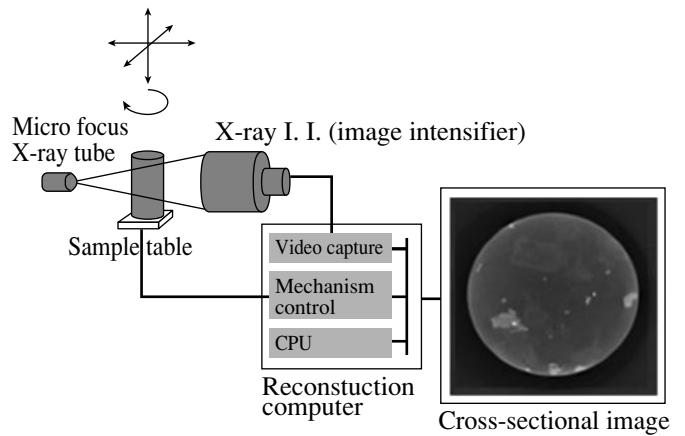


Fig. 2 A schematic diagram of the microfocus X-ray CT system.

tem. X-rays from microfocus X-ray generator are partially attenuated by a specimen that is made to rotate in equal steps in a full circle about a single axis close to its center. At each rotational position, the surviving X-ray photons are detected by an X-ray I. I. (Image Intensifier) large enough to contain the shadow of the specimen. These projection images are collected using conventional video technology. The video signal is then converted to a two-dimensional digital array by an image processing system. Finally, a three-dimensional image array is reconstructed from the collected set of projection images. The system can achieve 2048×2048 pixel reconstructions and obtain data needed for 3-D image in one scanning session. A high-resolution sensor and enhanced accuracy of image reconstruction software have achieved a spatial resolution of $5 \mu\text{m}$ and finer. In this study the system was used to observe microstructure of the rock specimens before and after a dynamic tensile test.

3. Dynamic tensile test and results

A dynamic tensile test based on Hopkinson's effect together with the spalling phenomena was used to observe a fracture plane position of the rock specimen subject to reflected tensile stress. Figure 3 shows a schematic of the dynamic tensile test. The test was commenced with a high-speed camera controller that simultaneously sends signals to the high-speed camera and the accurately controlled blasting machine, which sends an ignition signal to a precise electric detonator and the oscillograph of the laser vibration meter used to record oscillation. The rock specimen was shocked by the detonation of the precise detonator and the displacement velocity at the free end of the rock specimen was measured using a laser vibration meter. The mechanical properties and geometry of an Inada granite specimen are presented in table 1. Inada granite consists of quartz (34 % by volume), alkali-feldspar (24 %), plagioclase (33 %), biotite and other minerals (6 %). The mean grain size is about $2.0 \text{ mm}^{\text{a}}$.

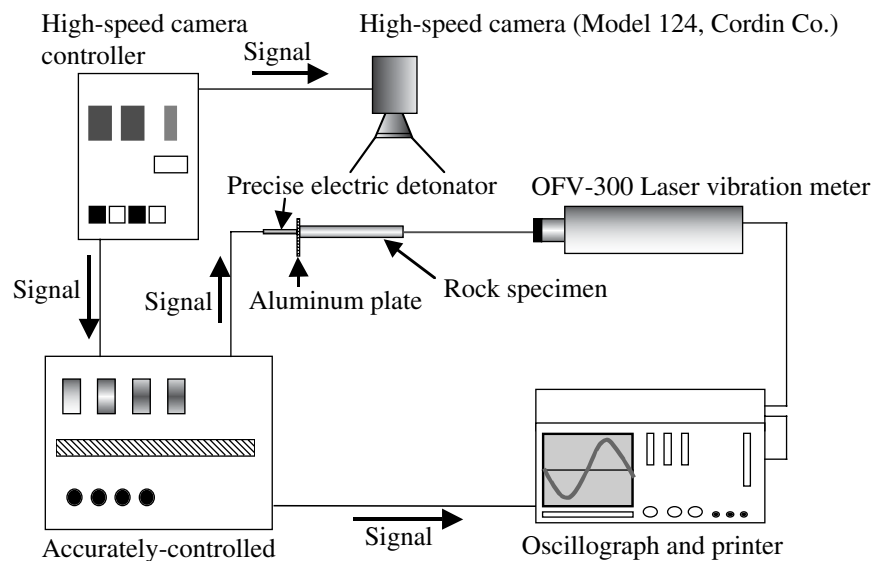


Fig. 3 Experimental set-up for the dynamic tensile test.

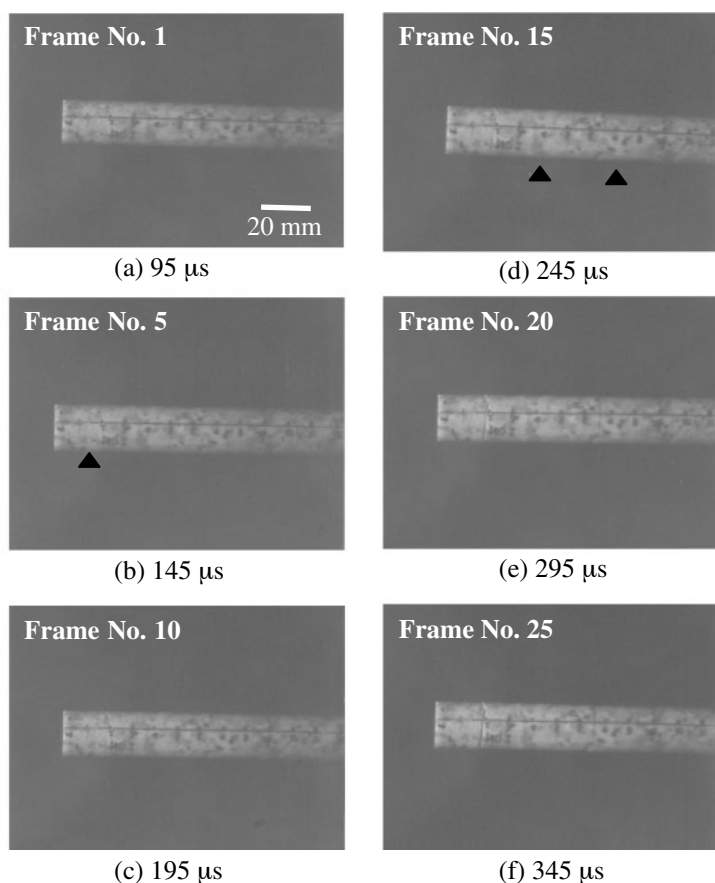


Fig. 4 Fracture process in an Inada granite specimen photographed using a high-speed camera.

Figure 4 shows high-speed framing photographs from frames 1 to 25. Triangles indicate the fracture planes that start to become visible. The fracture planes are located 20 mm, 35 mm and 65 mm from the free end. The first fracture that was formed stated to be visible when the collapsed time from the ignition of the detonator became 145 μ s.

Cho *et al.*³⁾ pointed out that large numbers of microcracks are generated under the applied tensile stress and fracture planes are formed due to the propagation and coalescence of the cracks. They confirmed that the experimental dynamic tensile test generated numerous cracks in test specimen

using an image photographed with fluorescent resin emitted light as shown in Fig. 5. The fracture plane is located 82 mm from the free end as indicated by a triangle. The cracks that have possible fracture planes are visible as indicated by arrows. The formation of fracture plane is influenced by various factors including the inhomogeneity of the rock, the stress rate and crack arrests. Therefore, to understand the effect of rock inhomogeneity on the fracture process of the rock subjected to dynamic tensile loading, it is necessary to observe the potential fracture planes in test rock specimen.

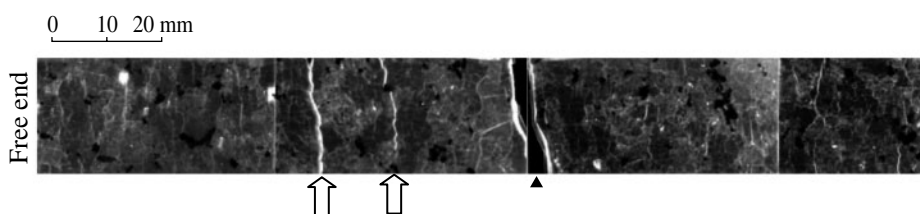


Fig. 5 Fracture plane and potential fracture planes in an Inada granite specimen photographed with fluorescent resin emitted light (after Cho *et al.*³⁾).

Table 1 Mechanical properties and geometry of an Inada granite specimen.

Exp. No.	Length (mm)	Diameter (mm)	Density (kg/m ³)	P-wave velocity (m/s)	Elastic modulus (MPa)
A-1	344	20	2600	3632	56.8

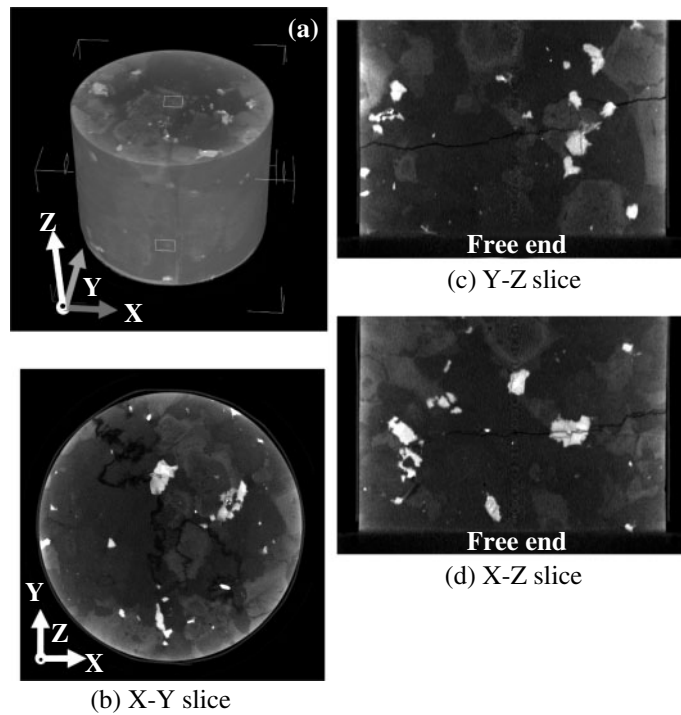


Fig. 6 3D structure of a region near the free end side in an Inada granite specimen (a) Volume-rendering image from 300 X-ray attenuation images, (b) Cross-sectional image of centre X-Y slice, (c) Selected cross-sectional image of centre X-Z slice, and (d) Selected cross-sectional image of centre Y-Z slice.

4. Microstructure visualization of test rock specimens and discussions

The Inada granite specimen was placed on the sample table and scanned by cone beam geometry X-ray generator covering 20 mm in diameter and 15 mm high before and after the dynamic tensile test. The scanning was conducted six times to observe the region from the free end to 90 mm length of the rock specimen. The source voltage and source current to accelerate the electrons were 90 kV and 89 μ A, respectively. The vertical slice width was 0.067 mm. The fragments of the test Inada granite specimen were reconstructed for the X-ray CT scanning.

Figure 6 (a) shows the volume-rendering 3D reconstruction image for the region near the free end side in the Inada granite specimen. The image set contains $1024 \times 1024 \times 687$ voxels (voxel resolution is 7.6 μ m). Figures 6 (b)-(d) show selected cross-sectional images of centre X-Y, X-Z and Y-X slices, respectively. Granite constituents and a

fracture plane parallel to the free end side are visible. The contrast in the images shows differences in the density of mineral; that is, the white portions indicate the places where high density minerals exist such as zirconium and biotite.

Figures 7 (a) and (b) show selected cross-sectional images that were generated using six X-Z and Y-Z slices for a total length of 90 mm, respectively. The triangles indicate the fracture planes observed by high-speed camera (Fig. 4). The arrow indicates the potential fracture plane which is not visible in Fig. 4. The selected cross-sectional images of the Inada granite specimen before the dynamic tensile test, as shown in Fig. 8, were then compared with that in Fig. 7 (a) and (b) to investigate blast-induced fractures in the Inada granite specimen. It is also examined whether there damage had occurred during the drill-hole coring. It was confirmed that no visible damage could be found in this resolution.

The potential fracture plane which is shown in Fig. 7 was enlarged using microfocus X-ray geometry as shown in

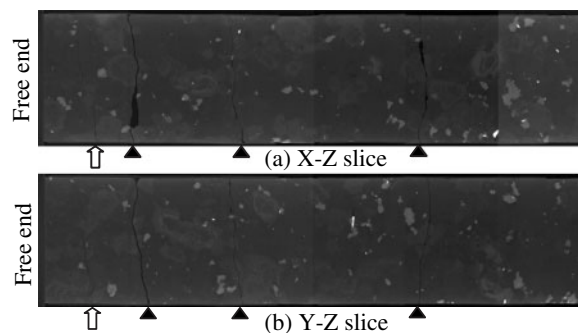


Fig. 7 Selected cross-sectional images in the tested Inada granite specimen.

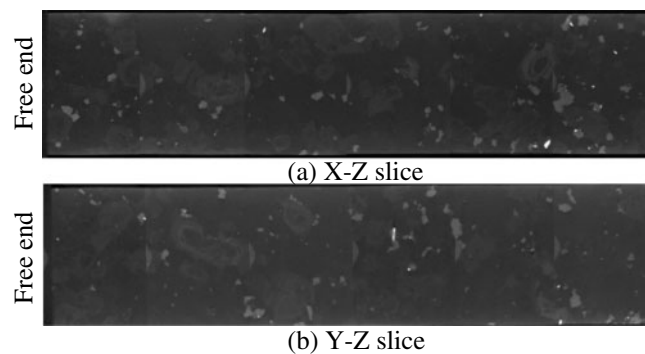


Fig. 8 Selected cross-sectional images in an Inada granite specimen before the dynamic tensile test.

Figs. 9. Numerous cracks that do not coalesce to form a single fracture plane are visible in Fig. 9 (b) and (c). Although the set of cracks is closest to the free end side, it is still unknown as to why the cracks do not coalesce to form the fracture plane. Cho *et al.*³⁾ revealed that a high strain rate increased the number of microcracks, which hindered the formation of the fracture plane due to the crack arrests caused by the stress released from adjacent microcracks. It can be easily conceived that the cracks which are seen in Fig. 9 (b) and (c) resulted from the interference of the formation of the fracture plane.

This study shows that micro X-ray CT system with a high spatial resolution is a useful tool for observing microcracks and internal structure of the rock specimen subject to dynamic loading.

5. Conclusions

A dynamic tensile test based on Hopkinson's effect together with the spalling phenomena was used to observe a fracture plane position of the rock specimen subject to

reflected tensile stress. The fracture planes were observed using high-speed camera.

The micro X-ray CT system was used to visualize 2D and 3D microstructure of the Inada granite specimen before the dynamic tensile test. The three fracture planes observed by high-speed camera and one potential fracture plane were observed from the selected cross-sectional images generated using six X-Z and Y-Z slices. The potential fracture plane was enlarged using microfocus X-ray geometry. Numerous cracks that do not coalesce to form a single fracture plane were observed and the reason as to why the cracks do not coalesce to form the fracture plane was discussed

References

- 1) G. Ma, A. Miyake, T. Ogawa, Y. Wada, Y. Ogata, M. Seto, and K. Katsuyama, 1998, Study on the tensile strength of brittle materials under high stress rate using the technique based on Hopkinson's effect. *J. Jpn Exp. Soc.*, 59(2): 49-56 [in Japanese].
- 2) Y. Wada, Y. Ogata, W. Jung, M. Seto, K. Katsuyama and T. Ogawa, 1999, Effect of water saturation and strain rate on the tensile strength of rocks under dynamic load. *Proc. '99 Japen-Korea Joint Symp. Rock Eng. Fukuoka, Japan*, 407-412.
- 3) S. H. Cho, Y. Ogata and K. Kaneko, 2003, Strain-rate dependency of the dynamic tensile strength of rock, *Int. J. Rock Mech. Min. Sci.*, 40: 763-777.
- 4) H. J. Vinegar, 1986, X-ray CT and NMR imaging of rocks, *J Pet Technol*, Vol. 38, No. 3, 257-259.
- 5) H. J. Vinegar, J. A. De Waal and S. L. Wellington, 1991, CT studies of brittle failure in Castlegate Sandstone, *Int J Rock Mech Min Sci Geomech Abstr* Vol. 28, No. 5, 441-447.
- 6) Otani, J., Mukunoki, T. and Obara, Y., 2000, Application of X-ray CT method for characterization of failure in soils, *Soils Found.*, 40, No. 2, 111-118.
- 7) C. L. Lin and J. D. Miller, 1996, Cone beam X-ray microtomography for three-dimensional liberation analysis in the 21st century, *Int. J. Miner. Process*, 47, 61-73.
- 8) J. D. Miller and C. L. Lin, 2003, 3-D analysis of particulates in mineral processing systems by cone beam X-ray microtomography, *Proceedings of 22th International Mineral Processing Congress*, 29, Sep. 2003, 1561-1570.
- 9) T. Takemura, M. Oda and M. Takahashi, 2004, Microscopic observation in deformed geomaterials using microfocus X-ray computed tomography, *X-ray CT for geomaterials; Soils, Concrete, Rocks*, Otani and Obara (eds.), Swets & Zeitlinger, Lisse, 2004, 299-304.

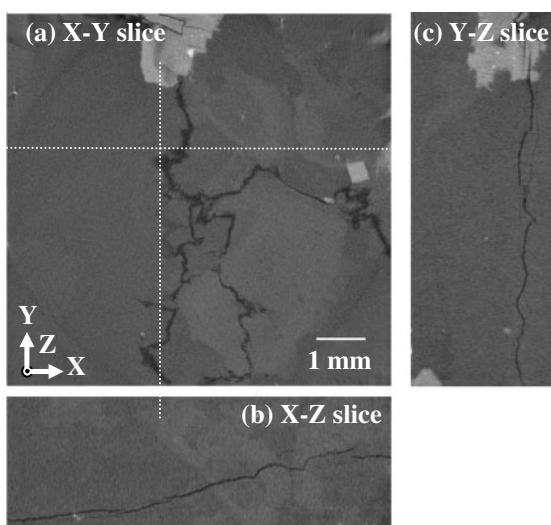


Fig. 9 Granite constituents and cracks identified from selected cross image of the 3D reconstruction of the tested specimen.

マイクロフォーカスX線CTを用いた 動的引張試験試料の観察について

趙 祥鎬^{**}, 久保田士郎^{**}, 緒方雄二^{**}, 横田光博^{*}, 金子勝比古^{*}

ホプキンソン効果による岩石の動的引張試験を行い、動的引張強度やそのひずみ速度依存性が評価されている。ホプキンソン効果による岩石の破断面形成は亀裂群の発生・連結および選択的成長という、複雑な過程を経ていることが確かめられた。破断面位置は動的引張強度の評価に使われるので、その破断面形成に関するメカニズムの解明は不可避である。本研究では、動的引張試験前後の岩石試料を観察するため、マイクロフォーカスX線CT(北海道大学、空間分解能5 μm)が用いられた。その結果、動的引張亀裂などに関する有益な情報を非破壊的に得ることが出来た。

*〒060-0813 札幌市北区北13条西8丁目 北海道大学 大学院工学研究科 環境フィールド工学専攻 地圏フィールド工学研究室 A6-55

†現：トロント大学土木工学専攻

†corresponding author: chosh@geo-er.eng.hokudai.ac.jp

**〒305-8565 茨城県つくば小野川16-1産業技術総合研究所、爆発安全研究センター